Desalination and Water Treatment
www.deswater.com

doi: 10.5004/dwt.2018.21910

104 (2018) 189–200
February

Research on nitrate removal from simulated groundwater by iron nanoparticle-loaded graphene

Yanhua Wang[a,b,*], Shengke Yang[b,*], Bin Li[b]

[a]*School of Geography and Tourism, Shaanxi Normal University, Xi'an, China, Tel. +86 13991828224; email: yhwang930@foxmail.com*
[b]*Key Laboratory of Subsurface Hydrology and Ecology in Arid Areas, School of Environmental Science and Engineering, Chang'an University, Xi'an, China, Tel. +86 15991655210; email: ysk110@126.com (S. Yang), Tel. +86 18049231762; email: 395820930@ qq.com (B. Li)*

Received 30 August 2016; Accepted 11 January 2018

ABSTRACT

Nitrate is one of the most frequent pollutants of groundwater, and in some areas, nitrate pollution is becoming a serious problem. While graphene has been widely used in the processing of heavy metal ions in aqueous solution, its role in nitrate removal remains largely unexplored. In this study, we loaded micro-sized graphene with nanoscale iron particles (G-Fe) by liquid-phase reduction. The characteristics of nitrate reduction by nanoscale zero-valent iron and G-Fe composites were determined under different conditions using static experiments, to reveal the reaction mechanism in removing nitrates. Under the same reaction conditions and dosing level, G-Fe achieved higher reaction rate and removal efficiency of nitrates, with a lower production rate of ammonia. Results show that the optimal load ratio of graphene with nanoscale iron is 5:1. Lower initial pH improves nitrate removal efficiency (NRE) to varying degrees and 100% removal is obtained at pH 2.15. Dissolved oxygen has no effect on NRE. The effect of coexisting anions on NRE descends as follows: PO_4^{3-}, SO_4^{2-}, and Cl^-. Kinetic studies show that the reaction order between G-Fe and nitrate is about 0.45, indicating that the reaction involves complex redox reactions and adsorption/desorption processes, other than a simple first-order reaction. This study demonstrates the effectiveness of G-Fe composites in nitrate removal and establishes an advanced technology for groundwater remediation.

Keywords: Micro-sized graphene; Nanoscale zero-valent iron; Groundwater; Nitrate removal; Kinetic reaction mechanism

1. Introduction

Groundwater is an important water body in a close relationship with human society. Owing to high levels of urbanization, increased population growth, and industrial development, surface water pollution is becoming a growing issue worldwide. This has led to an increase in the number of people depending on groundwater for domestic and drinking water [1–3]. However, excessive nitrogen use in agriculture, unreasonable nitrogen emission from residential and industrial wastewater, and extreme treatment and discharge of livestock farm wastewater, have all led to nitrates polluting groundwater, which can seriously influence both groundwater environment and human health.

The literature reports that in more than 100 sites of Wales in England, groundwater nitrate concentrations were significantly higher than drinking water standards, directly affecting an area of more than 1,800,000 people [4]. According to a groundwater quality survey by the US environmental protection department in 1992, about three million residents, including more than 43,500 children, exceeded nitrate concentrations in their drinking water. Moreover, nitrate has become a major groundwater contaminant in the USA, with the average annual growth of groundwater nitrate levels in many areas being 0.8 mg/L [5,6]. In France, Russia, and Netherlands, nitrate groundwater concentrations have been recorded at 40–50 mg/L, sometimes even up to 500–700 mg/L [7].

* Corresponding author.

1944-3994/1944-3986 © 2018 Desalination Publications. All rights reserved.

Nitrates have been frequently present in drinking water and various types of agricultural, domestic, and industrial wastewater [8,9]. Their presence has been linked to several environmental problems. For example, nitrates can stimulate eutrophication where pollution is caused in waterways by heavy algal growth, as nitrogen is a rate-limiting nutrient for the process. Additionally, nitrate contaminated water supplies have been linked to outbreaks of infectious disease [10]. While, high concentration of nitrates in drinking water can lead to the formation of nitrosoamine, which is related to cancer and increased risk of diseases such as methemoglobinemia in newborn infants [8,11–13]. Rapid population growth and increased demand for food have caused water nitrate pollution to become a global scope for serious environmental problems [2,14]. Hence, research into the theories and methods of nitrate pollution control in groundwater is of important theoretical value and practical significance.

Since 1960s, there has been extensive focus placed on researching groundwater nitrate pollution and remediation technology. Existing technologies for the remediation of nitrate contaminated groundwater can be roughly divided into three types: bioremediation (e.g., biological denitrification [15]), physical and chemical remediation (e.g., ion exchange method [16,17]), and chemical remediation (e.g., catalytic reduction [18] and including electrochemical reduction method [19]). The chemical method is generally better than the commonly used biological and physical methods for removing nitrates. Advantages of the chemical method include no secondary pollution, high efficiency, simple processing facilities, and small size [20]. In particular, the active metal reduction method has features including being a metal reducing agent, inexpensive, and exhibiting high removal efficiency [18]. As such, it has acquired universal attention by researchers in recent years.

Metal iron has become one of the most studied reducing agents. Li et al. [21] previously used reducing iron powder to remove nitrates from groundwater. They showed that while at pH 2 the removal efficiency was more than 90%, under neutral conditions the reduced iron powder did not react with nitrates. Nanoscale zero-valent iron (NZVI), with its great surface area and strong activity, has unique advantages and good application prospects in groundwater pollution remediation. Li et al. [22] demonstrated nitrate removal with NZVI prepared by liquid-phase reduction, with removal rate reaching 90% (at Fe/N ratio of 50:1). However, the dosing amount of NZVI is large and the initial rate of nitrate reduction reaction (NRR) is not high. Moreover, NZVI does not adapt well to the high concentrations of nitrate pollution remediation [7]. Alternatively, NZVI can be fixed onto certain carriers to effectively prevent the agglomeration of particles, thereby improving the reaction activity and selectivity of nitrogen [23].

Graphene, a two-dimensional carbon nanomaterial and the fundamental building block of graphite, provides a large surface area (2,630 m^2/g), with excellent electrical, thermal, and mechanical properties [24,25]. It can be easily prepared from cheap natural graphite [24], and has demonstrated to be a promising adsorbent in removing heavy metals from aqueous solution, for example, uranium [26,27], chromium [28], thorium [29], and antimony [30]. Additionally, graphene exhibits exciting adsorption abilities for removing hazardous cationic dyes such as methylene blue and safranin T from contaminated water [27,30]. Graphene oxide (G) can be also easily prepared by several classical methods from cheap natural graphite, introducing oxygen-containing functional groups such as carboxyl and hydroxyl groups into carbon sheets [25–27]. While graphene has been widely used in the processing of heavy metal ions in aqueous solution, its role in nitrate removal remains largely unexplored.

In this study, we conducted static experiments of removing nitrates using graphene loaded with iron nanoparticles (G-Fe). The objectives of the study were to: (1) assess the effects of graphene load, initial concentrations of NO_3^-, pH, dissolved oxygen (DO), and coexisting anions on the nitrate removal efficiency (NRE); and (2) reveal the reaction mechanisms involved in G-Fe composites removing nitrates. The results provide reference data for engineering application of nitrate removal technology in the water.

2. Materials and methods

2.1. Materials

We purchased graphene oxide (G) from the Chinese Academy of Sciences, Chengdu Institute of Organic Chemistry Co. Ltd. (Chengdu, China); potassium borohydride (KBH_4) and polyethylene glycol (PEG 4000) from Tianjin Kermel Chemical Reagent Co. Ltd. (Tianjin, China); anhydrous ethanol from Tianjin Fuyu Chemical Co. Ltd. (Tianjin, China); and ferrous sulfate heptahydrate ($FeSO_4 \bullet 7H_2O$) from Xi'an Chemical Reagent Factory (Xi'an, China). All chemicals were analytically pure and prepared in deoxygenated distilled water for all experiments.

2.2. Preparation of composites

2.2.1. Preparation of NZVI

NZVI was prepared by liquid-phase reduction. Briefly, $FeSO_4 \bullet 7H_2O$ and PEG 4000 were dissolved in 10 mL of distilled water under nitrogen protection. When the chemicals were completely dissolved, followed by addition of 20 mL of anhydrous ethanol. With vigorous stirring under nitrogen protection, 20 mL of 1 mol/L KBH_4 solution was slowly added dropwise. After 30 min of reaction, the materials were washed three times with distilled water, before rewashing three times with anhydrous ethanol. NZVI prepared was stored in anhydrous ethanol until used (Fig. 1).

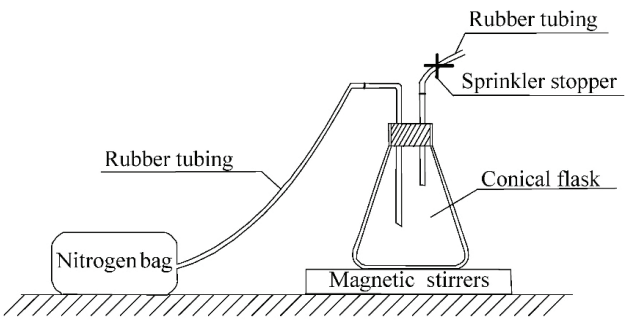

Fig. 1. Schematic diagram of the device to prepare graphene loaded with iron nanoparticles.

2.2.2. Preparation of G-Fe composites

G-Fe was prepared by liquid-phase reduction [22]. Briefly, $FeSO_4 \bullet 7H_2O$ and PEG 4000 were dissolved in 10 mL of distilled water under nitrogen protection. When the chemicals were completely dissolved, graphene was added with continuous stirring, followed by addition of 20 mL of anhydrous ethanol. With vigorous stirring under nitrogen protection, 20 mL of 1 mol/L KBH_4 solution was slowly added dropwise. After 30 min of reaction, the materials were washed three times with distilled water, before rewashing three times with anhydrous ethanol. These composites were stored in anhydrous ethanol until used (Fig. 1).

2.2.3. Preparation of nitrate solution

All the glassware used in the experiment was soaked overnight in a 10 mg/L of NO_3^- solution to minimize the possibility of NO_3^- being adsorbed on glass surface during experimental work. Then, the glassware used is washed several times with distilled water. KNO_3 is used as a source of nitrate. Stock solution of NO_3^- was prepared by dissolving KNO_3 in double distilled water having NO_3^-. Also, the analyses were performed in duplicate.

2.3. Nitrate removal experiments

Nitrate removal experiments were carried out in a 250-mL airtight custom-made reaction vessel (Fig. 2). The reaction temperature was 25°C and the oscillation strength was 150 rpm. A parallel experiment was conducted using NZVI or G-Fe, respectively, with the initial NO_3^- concentration of 50 mg/L. The removal experiment was carried out at 25°C ± 0.1°C. Water samples were obtained at different time points through a 10-mL syringe inserted to the plug of reaction vessels. At the given time intervals, 3.5 mL of solution sample were withdrawn and filtered through a 0.22 μm membrane and stored in 25-mL colorimetric tubes before testing. Water samples were collected at regular intervals to measure nitrate, nitrite, and ammonia concentrations.

For chemical analysis, nitrate was determined by UV spectrophotometry [7,21] and ammonia determined by Nessler's reagent spectrophotometry [22,23]. And N-(1-nky)-ethylenediamine spectrophotometric method was used to determine nitrite nitrogen [23]. The NRE (%) was calculated using the following equation:

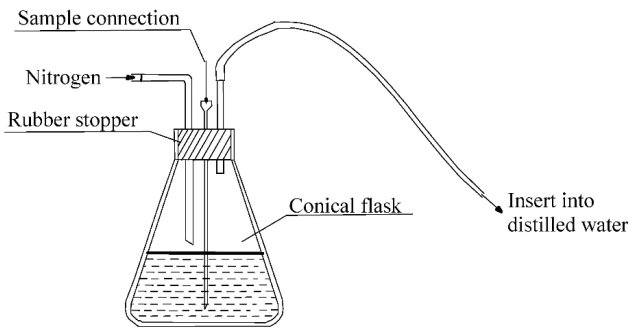

Fig. 2. Schematic diagram of custom-made reaction vessel for nitrate removal experiments.

$$\eta = \frac{C_0 - C}{C_0} \times 100\% \tag{1}$$

where C_0 is the initial NO_3^- (NH_4^+) concentration and C is the constant NO_3^- (NH_4^+) concentration.

2.4. Characterization

The morphology of G-Fe was observed before and after reaction (0, 30, and 90 min). The samples were cleaned multiple times with anhydrous ethanol and air-dried under nitrogen. A small amount of samples was examined by scanning electron microscopy (SEM) [31]. X-ray diffraction (XRD) was carried out on a Bruker D8 Advance X-ray diffraction instrument with a step size of 0.02°, and the diffraction angle (2θ) from 5° to 90° was scanned [27]. The BET data of graphene, NZVI and G-Fe such as porosity and surface area was acquired by specific surface area analyzer (KUBO-1108).

2.5. Kinetic studies

The reaction kinetics as a function of nitrate concentration can be represented as [32]:

$$r = \frac{-dC}{dt} = k\left[Fe\right]C^n \tag{2}$$

A nitrate concentration curve was plotted against time (the kinetic curve) and then used to calculate dC/dt of different reaction times. Because iron is a solid phase, k[Fe] can be thought of as a constant, k_{obs}; the resulting equation is as follows:

$$r = \frac{-dC}{dt} = k_{obs} \cdot C^n \tag{3}$$

where r (mg NO_3^--N/L min) is the NRR, k [(mg-N/L)$^{1-n}$• L/m^2 min] is the NRR constant, k_{obs} [(mg-N/L)$^{1-n}$/min] is the apparent NRR constant; C (mg-N/L) is the nitrate concentration, t (min) is the reaction time, and n is the reaction order.

Taking the logarithm of both sides of the upper formula was:

$$\ln r = \ln\left(\frac{-dC}{dt}\right) = \ln k_{obs} + n \cdot \ln C \tag{4}$$

Plots were established with ln$C$ as the abscissa and lnk_{obs} as the ordinate. The experimental data were fitted to the equation using Origin 8.0 (OriginLab Corp., Northampton, MA, USA). The obtained reaction order n, apparent rate constant k_{obs}, and correlation coefficient R^2 were used for kinetic analysis.

3. Results and discussion

3.1. Nitrate removal by NZVI

3.1.1. Removal effect of NZVI and product analysis

The results show that NRE in simulated groundwater reached 86% after 90 min of reaction with NZVI at pH 2

(Fig. 3(A)). As can be seen, NZVI has a strong capacity for nitrate reduction under acidic conditions. Owing to its high reduction activity, NZVI can reduce nitrates into ammonium, nitrogen, and nitrite at the cost of oxidizing itself to ferrous iron [7]. Ammonium is the major product of nitrate reduction and its production rate ultimately reached 95% in the experiment (Fig. 3(B)). Nitrite is only a transient intermediate produced during the reduction reaction. It has been reported that nitrite concentrations first increased to the peak level with extended time of reaction, and then followed a decreasing trend thereafter; no nitrite was detected in the aqueous solution at the end of the reaction.

Research indicates that the reaction of nitrate removal by NZVI follows first-order reaction within the range of 30–120 mg/L initial NO_3^- [7]. We fitted the kinetic equation using the experiment data and found that the reaction of nitrate removal was conformed to pseudo-first-order reaction at 50 mg/L initial NO_3^-. With increasing dose of NZVI, the k_{obs} value became increasingly greater (Table 1). Under the same conditions of initial NO_3^- concentration and reaction volume, an increased dose of NZVI results in a higher mass ratio between NZVI and nitrate ions. Thus, a higher level of excess NZVI results in a greater k_{obs} value [7,21].

In addition, to test the effect of NZVI dosage on nitrate removal, we prepared NZVI and nitrate at different mass ratios (5:1, 10:1, 20:1, 40:1, and 60:1) and monitored their reaction with nitrate for 1 h. When the initial concentration of NO_3^- was 50 mg/L and pH = 2. Research indicates that the optimal mass ratio of NZVI and nitrate was 40:1. Therefore, we chose it as the optimal condition in the following experiments.

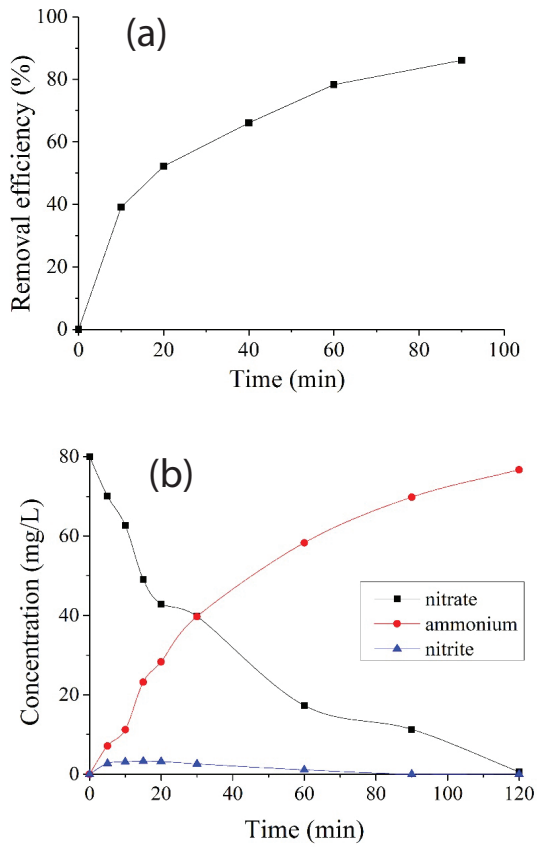

Fig. 3. Nitrate removal efficiency (A) and ammonia production rate (B) by nanoiron in simulated groundwater. (A) Initial nitrate concentration = 50 mg/L, pH = 2.0, and NZVI (1.33 g/L Fe). (B) Initial nitrate concentration = 80 mg/L, pH = 2.0, and NZVI (1.33 g/L Fe).

3.1.2. Effect of initial NO_3^- concentration on NRE

Effect of initial NO_3^- concentration (30, 50, 80, and 120 mg/L) on removal of nitrate by NZVI is shown in Fig. 4. As revealed, it was shown similar reaction trends that different initial concentrations of nitrate solution reacted with NZVI. In the experimental condition, the removal rate of the nitrate was decreased with the increasing of initial NO_3^- concentration. With the increase of reaction time, the corresponding removal rate showed a significant downward trend. This is because the removal of nitrate is accompanied by the formation of iron oxide and hydroxide, resulting in the passivation of NZVI surface and reducing the rate of reaction [13]. Meantime, the nanoparticles could reunited in the reaction process, which led to reduce the activity of the reaction. Therefore, as the reaction progressed, the reaction rate decreased, and the removal rate of the corresponding time reduced. NZVI removal mechanism was used to adsorb the nitrate, and then chemical reaction on its surface. Which lead to that nitrate had been converted into nitrogenous nitrogen, ammonia nitrogen, and some nitrogen. When the nitrate concentration is low, NZVI is relatively excess, and the nitrate could be fully adsorbed and reacted [11]. However, when the nitrate concentration is high, the adsorption capacity of NZVI is relatively insufficient, and the removal rate of nitrate is also low [13].

Table 1
Fitting of kinetic equations for reaction between NZVI and nitrate in simulated groundwater

NZVI (g)	k_{obs} (min^{-1})	Rate equation
0.20	0.015	$\ln(C/C_0) = -0.015 \times t$
0.25	0.019	$\ln(C/C_0) = -0.019 \times t$
0.50	0.036	$\ln(C/C_0) = -0.036 \times t$

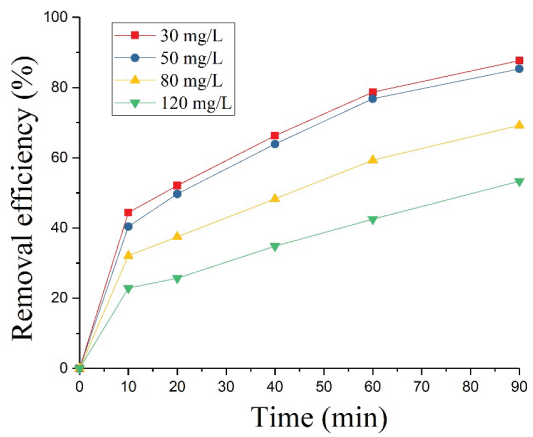

Fig. 4. Reaction of NZVI with different initial concentration NO_3^- solution.

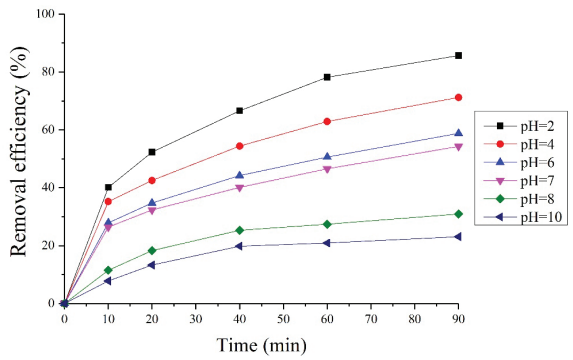

Fig. 5. Influent of different pH values on NRE by NZVI.

3.1.3. Effect of pH on NRE

The pH value was an important factor affecting NZVI reduction of nitrate. To examine the effect of pH on the NRE of NZVI, we conducted batch experiments at a wide range of pH value (pH = 2, 4, 6, 7, 8, and 10), the mass ratio of NZVI and nitrate was 40:1, and the initial concentration of NO_3^- was 50 mg/L. The reaction concentration was measured at different reaction times. As revealed in Fig. 5, when the pH value of the solution was 2.0, the removal effect was the best. With the increasing pH, the removal rate gradually decreased. When the pH value of the solution was 10.0, the maximum removal rate of nitrate solution was only about 20% after reaction equilibrium. This indicated that the reduction of nitrate by NZVI had been an acidic driving reaction [13]. The lower the pH value of groundwater, the more favorable the reaction of elemental iron and nitrate. This is due to that zero-valent iron had easily converted into iron ions in the reaction [6,7]. As depicted in the follow equation:

$$Fe^0 + 2H_2O \rightarrow Fe^{2+} + H_2 + 2OH^- \quad (5)$$

Simultaneously, zero-valence iron also has a reaction with nitrate:

$$5Fe^0 + 2NO_3^- + 6H_2O \rightarrow 5Fe^{2+} + N_2 + 12OH^- \quad (6)$$

Under the acidic conditions, nitrate can be reduced by zero-valent iron, the reaction equation is as follows:

$$Fe^0 + NO_3^- + 2H^+ \rightarrow Fe^{2+} + H_2O + NO_2^- \quad (7)$$

In the alkaline environment, zero-valent iron is easy to generate $Fe(OH)_2$ and $Fe(OH)_3$. Zero-valent iron is also likely to generate some ferrous hydroxide complex ions such as $[Fe(OH)]^+$, $[Fe(OH)_3]^-$, $[Fe(OH)_4]^{2-}$, and $[Fe(OH)_4]^{2+}$ [6]. It will reduce the reactant concentration. There are double effects of adsorption and reduction in the experiment of NZVI removal of nitrate and therefore the pH value of the solution has a great effect on the reaction [7,13].

3.1.4. Effect of DO on NRE

The removal efficiency of nitrate was investigated under aerobic and anaerobic situation, respectively. The results are illustrated in Fig. 6. As revealed, for NZVI treatment, 67.2% of nitrate was reduced in the anaerobic system, but the removed

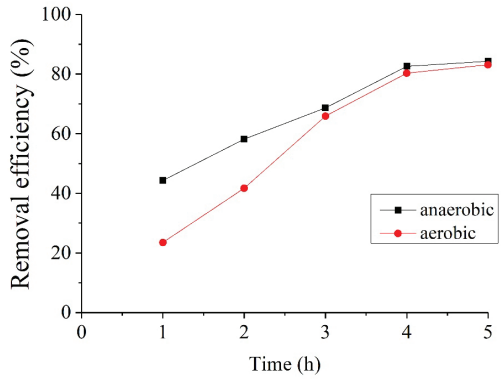

Fig. 6. Effects of DO on NRE by NZVI under anaerobic and aerobic situation.

percentage accounted for only 39.7% in the aerobic system within 3 h. When DO is contained in solution, the removal rate of nitrate is reduced. However, after 3 h, there was no significant difference in the removal rate of nitrate under the two conditions. This may be due to aerobic conditions, the oxide formed on the surface of iron powder has a certain inhibiting effect on the reaction process [19]. The DO played a role of electron acceptor and competed with nitrate in the reaction, as depicted in the follow equation:

$$2Fe^0 + 2H_2O + O_2 \rightarrow 2Fe^{2+} + 4OH^- \quad (8)$$

With the progress of the reaction, the oxygen in the solution gradually had been consumed, therefore, the two groups of tests on NRE tends to be the same after 3 h. The presence of oxygen easily formed an oxide film on the iron surface, which made the iron particles passivated [23,27]. However, NZVI had a strong ability to supply electrons. In the actual experiment, the effect of DO on the removal rate is not significant [19].

3.1.5. Effect of coexisting anions on NRE

A large number of ions are present in groundwater, including K^+, Ca^{2+}, Mg^{2+}, Na^+, Cl^-, SO_4^{2-}, and PO_4^{3-}. Cations (e.g., K^+, Ca^{2+}, Mg^{2+}, and Na^+) have no effect on nitrate removal, while anions (e.g., Cl^-, SO_4^{2-}, and PO_4^{3-}) can affect NRE to varying degrees [22,33]. In this study, batch experiments were conducted to assess the effect of anions on NRE. In real systems several other ions are present which can compete with nitrate. The effects of presence of chloride, sulfate, and phosphate ions on nitrate removal were studied. As can be seen in Fig. 7, Cl^-, SO_4^{2-}, and PO_4^{3-} had a significant effect on nitrate removal, especially sulfate and phosphate ions. This may be because these two anions are involved in the corrosion reaction of NZVI, competing with NO_3^-–N for the reaction sites. Which inhibited the removal of nitrate in groundwater to some extent [13,19].

3.2. Nitrate removal by G-Fe

3.2.1. Effect of graphene dosage on NRE

The carrier dosage of G-Fe may affect the activity of the composites and the products of nitrate reduction [7]. To test

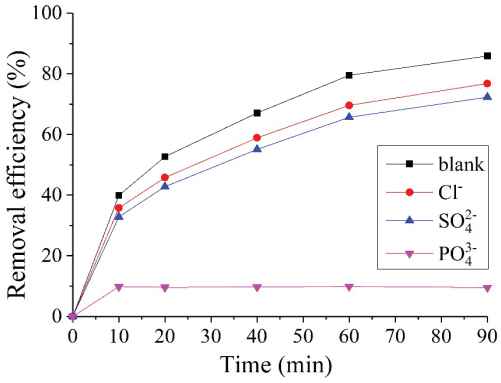

Fig. 7. Effects of coexisting anions on NRE by NZVI.

the effect of graphene dosage on nitrate removal, we prepared G-Fe at different load ratios (2.5:1, 5:1, 7.5:1, and 15:1) and monitored their reaction with nitrate for 30 min.

Fig. 8(A) shows that when the load ratio was greater than 7.5:1, there was an obvious decline in NRE. At higher load ratios, the reunion of graphene possibly coats the NZVI inside the aggregate, affecting the reduction reaction [22]. When the load ratio of graphene and NZVI was 5:1 or lower, more than 90% nitrate was removed within 30 min. At this point, both the dispersion and quantity of NZVI on the surface of the graphene may be satisfactory, resulting in the fastest reduction of nitrate.

Additionally, an increased dosage of graphene resulted in a decreased production of ammonia nitrogen (Fig. 8(B)), while the NRE decreased from 95.6% to 65.3% (Fig. 8(A)). Taking into consideration the nitrate removal and ammonia production, we chose the load ratio of graphene and NZVI at 5:1 as the optimal condition in the following experiments.

3.2.2. *Effect of initial NO_3^- concentration on NRE*

Since groundwater pollution with nitrate may occur at varying levels, we determined the NRE of G-Fe at different initial concentrations of NO_3^-. Fig. 9 demonstrates that when the initial concentration of NO_3^- was 50 mg/L or lower, G-Fe removed 100% of nitrates within 90 min of reaction. It can be seen when the mass ratio of iron and nitrogen is 30:1, G-Fe achieve the highest NRE. Moreover, nitrate removal by G-Fe (1.5 g/L Fe) resulted in a much less production of ammonium (67.1%) compared with that from nitrate removal by NZVI (3.33 g/L, 96.1%).

Under the experimental conditions, there was excess G-Fe in the reaction system. Within the same reaction time, NRE decreased with increasing initial concentration of NO_3^-. On the other hand, the removal rate followed a markedly decreasing trend with increasing reaction time. The process of nitrate removal is associated with production of iron oxides and hydroxides, leading to surface passivation of the composite material [22,32]. This mechanism reduces the reaction activity of the material and thus decreases the removal rate over time or NRE within the same reaction time.

3.2.3. *Effect of pH on NRE*

Research indicates that ordinary iron powder easily removes nitrate under acidic conditions, while under neutral

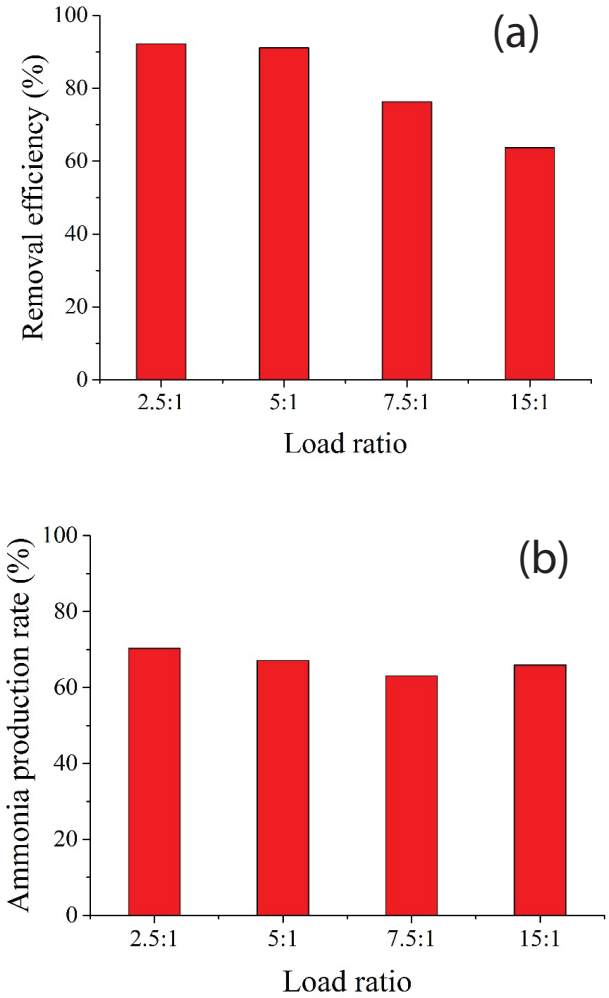

Fig. 8. Effect of load ratio of graphene and iron nanoparticles on nitrate removal efficiency (A) and ammonia production rate (B) in simulated groundwater. (A) Initial nitrate concentration = 50 mg/L, pH = 2.0, and G-Fe (1.5 g/L Fe). (B) Initial nitrate concentration = 50 mg/L, pH = 2.0, and G-Fe (1.5 g/L Fe).

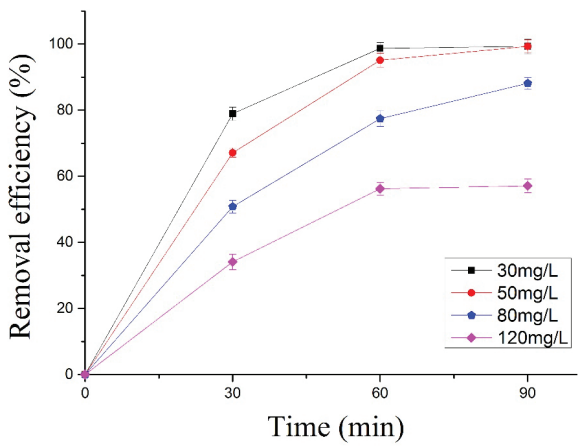

Fig. 9. Effect of initial NO_3^- concentration on removal efficiency of nitrates by graphene loaded with iron nanoparticles in simulated groundwater.

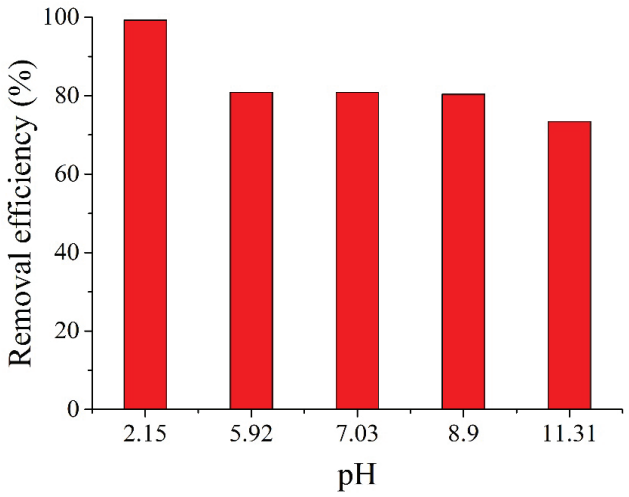

Fig. 10. Effect of pH on removal efficiency of nitrates by graphene loaded with iron nanoparticles in simulated groundwater.

conditions, the reaction is slow [21]. To examine the effect of pH on the NRE of G-Fe, we conducted batch experiments at a wide range of pH (2.15–11.31).

As can be seen in Fig. 10, when the pH was 2.15, NRE reached 100%. At pH 5.92, 7.03, and 8.90, respectively, the NRE values were all above 80%. Even at pH 11.31, NRE remained at 75.4%. Clearly, the NRE of G-Fe decreases with increasing pH in simulated groundwater. The results suggest that the reduction reaction of nitrates by G-Fe is acid responsive. Similarly, as observed on NZVI, the NRE declined from 57.3% to 31.5% while pH increased from 4 to 6 [34].

Low pH is advantageous to surface erosion of G-Fe and subsequent release of hydrogen, providing more adsorption sites and thus enhancing nitrate removal [22,34]. Under neutral condition, H^+ and adsorption sites are relatively few, affecting nitrate removal. Under alkaline conditions, excessive OH^- may form a passivation film deposited on the surface of the G-Fe composites, which prevents their contact with nitrates and thus reduces nitrate removal. Likewise, other study reported that the pH effect was significant for nitrate removal by zero-valent iron packed columns; the NRE decreased with increasing pH [21,22,27].

3.2.4. Effect of DO on NRE

Since NZVI has a strong reducing function, DO in groundwater may react with it as electron acceptors, forming the competition with nitrate reduction. Such reactions in theory would slow the removal rate of nitrate [35,36]. To find out the influence of DO on NRE, we added G-Fe to water samples containing different concentrations of DO, and monitored nitrate removal for 90 min.

As illustrated in Fig. 11(A), DO did not seem to greatly impact the final NRE, and 100% of nitrates were removed after 90 min of reaction. The possible reasons were: (1) The NZVI content possibly exceeded the amount required for nitrate removal, causing DO to be consumed by the NZVI, which would influence minimal nitrate removal [26,33]. (2) The removal process of nitrates produced N_2, which

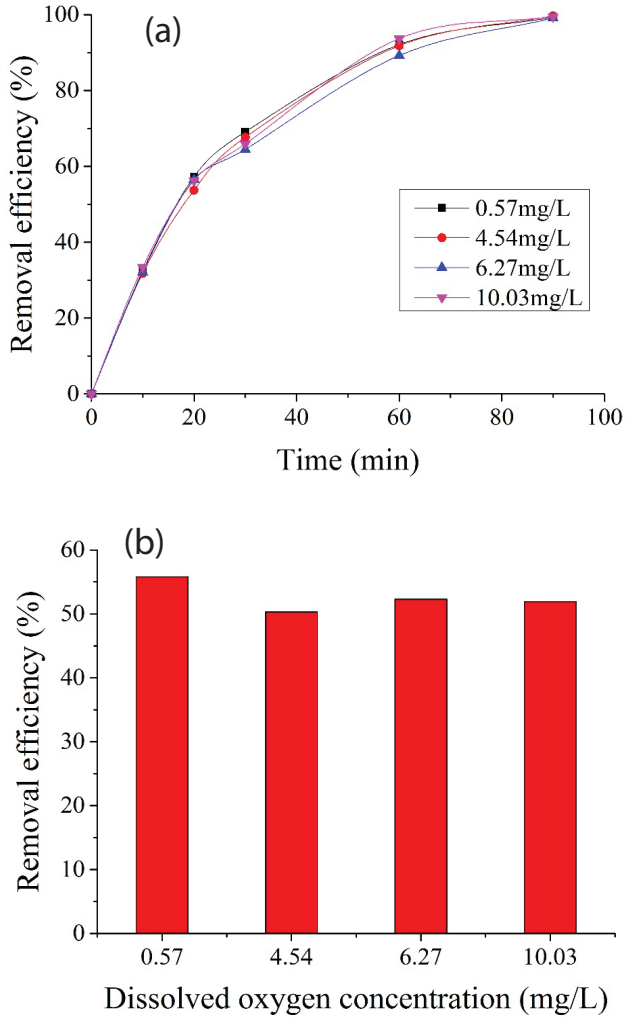

Fig. 11. Effect of dissolved oxygen on removal efficiency of nitrates by graphene loaded with iron nanoparticles in simulated groundwater in 90 min of reaction (A), with the greatest effect at 20 min (B).

would displace DO [32]. The DO levels produced certain effect over the reaction, with the greatest effect at 20 min (Fig. 11(B)). The results suggest that low DO levels were more conducive to nitrate removal. The NRE remained fairly constant at DO concentrations greater than 4.54 mg/L. However, previous research on nitrate removal by other materials had found that DO strongly affects the NRE. For example, when NZVI was applied in the same reaction conditions, 62.3% of nitrate was reduced in the anaerobic system and the NRE dropped to 22.1% in the aerobic system within 120 min of treatment [7].

3.2.5. Effect of coexisting anions on NRE

Fig. 12 shows that the effect of different anions on NRE can be sorted as follows: $Cl^- < SO_4^{2-} < PO_4^{3-}$. The greatest effect of PO_4^{3-} resulted in the lowest NRE being less than 10%. PO_4^{3-} possibly formed a complex compound with the NZVI, causing a reduction in its reactivity and subsequently a dramatic loss of NRE. In order to ascertain the effect of PO_4^{3-}, we set

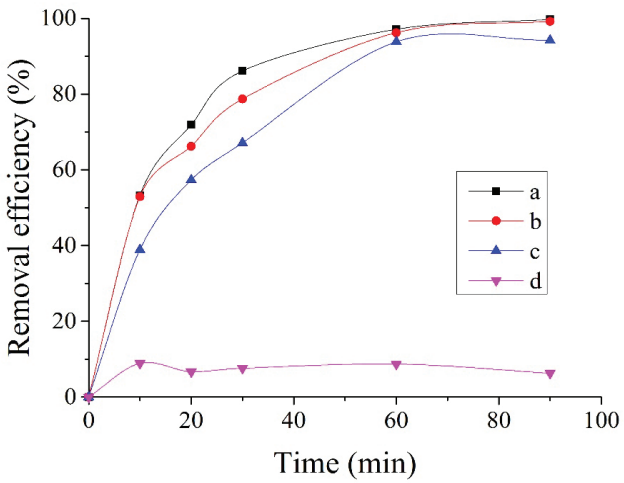

Fig. 12. Effect of coexisting anions on removal efficiency of nitrates by graphene loaded with iron nanoparticles in simulated groundwater (a) 50 mg/L NO_3^-, (b) 50 mg/L NO_3^- + 200 mg/L Cl^-, (c) 50 mg/L NO_3^- + 200 mg/L SO_4^{2-}, and (d) 50 mg/L NO_3^- + 50 mg/L PO_4^{3-}.

up parallel experiments of nitrate removal in the presence of PO_4^{3-} using graphene and G-Fe, respectively. After 90 min of reaction, graphene only adsorbed a small proportion (4.42%) of PO_4^{3-}, whereas G-Fe removed most (76.83%) PO_4^{3-} from the solution. Graphene only absorbed a small amount of PO_4^{3-} and most of PO_4^{3-} was removed by G-Fe. PO_4^{3-} and NZVI generated complex, which made NZVI lose its reactivity, resulting in nitrate removal rate dropped significantly below 10%. The results indicate that PO_4^{3-} competes with NO_3^- for the adsorption sites on the surface of G-Fe, thus reducing NRE. Pretreatment of PO_4^{3-}-containing groundwater is necessary before nitrate removal in practice. Obviously, the effect of G-Fe removal of nitrate was significantly better than NZVI. We selected G-Fe as the study object in the following experiments.

3.3. Characterization study

3.3.1. BET study

In this study, the specific surface area of the material (NZVI, graphene, and G-Fe) was measured by nitrogen adsorption–desorption analyses. The samples were degassed at 200°C for 12 h, and the temperature of liquid nitrogen was 77 K. The surface area of NZVI, graphene, and G-Fe was 35.76, 103.63, and 158.32 m^2/g. It can be seen that the composite adsorbent has a larger specific surface area relative to the other two materials.

3.3.2. XRD study

XRD pattern is shown in Fig. 13. The characteristic peak at 23° was the characteristic diffraction peak of graphene and the sharp diffraction peak at 10.6° was characteristic peak of graphene oxide. When graphene oxide was reduced, the diffraction peak at 10.6° diminished and eventually disappeared. However, the diffraction peak at 23° had become higher. It showed that graphene oxide is reduced to grapheme

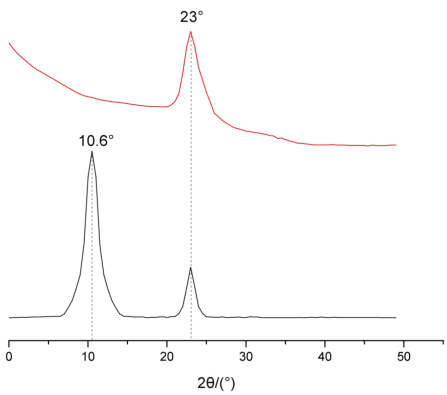

Fig. 13. XRD patterns.

3.3.3. SEM study

In order to explore the reaction mechanisms of nitrate reduction, we observed G-Fe samples at 0, 30, and 90 min of reaction. SEM analysis revealed the presence of black sheets (graphene) up to a few dozen microns in size, and white granules (NZVI particles) about 20–80 nm in size, in the composite samples before reaction. NZVI was distributed in clusters on the surface and within the gaps of the graphene sheets (Fig. 14(A)).

After 30 min of reaction, NZVI morphology varied from granular to flocculent, and the reaction product covered the graphene surface. The adhesion formed between graphene sheets and the NZVI particles were dispersed on the surface of the graphene sheets, including more unreacted granular NZVI (Fig. 14(B)). After 90 min of reaction, the graphene sheets were covered completely by the floc generated, in the absence of unreacted granular NZVI (Fig. 14(C)). The prepared G-Fe composites can quickly remove nitrate under specific conditions, owing to the large specific surface area, strong adsorption, and high surface reaction potential [7,26,27].

3.4. Reaction kinetics

The reaction of G-Fe with nitrates involves both reduction and adsorption processes, making it more complex than a simple first-order reaction model. Therefore, we adopted kinetics studies on the reaction, simulated a dynamic equation based on the measured data, and assessed the effects of different environmental factors on the NRR.

As shown in Table 2, ln$C$ and ln$r$ exhibit a good linear correlation at different graphene loads, with R^2 close to or greater than 0.95 at n = 0.38–1.08. When the load ratio was greater than 5.0, the k_{obs} value decreased visibly. An increase in graphene load also caused the NRR to decrease gradually.

In order to examine the effects of the reaction conditions on NRR, we used the reaction equation fitting from above to carry out kinetic analysis [22,31]. The optimal load ratio of graphene and NZVI was 5:1. Thus, we took the reaction order n = 0.45 to give the kinetic equation: $-dC/dt = k_{obs} \times C^{0.45}$. Integral: $C^{0.55} - C_0^{0.55} = -0.55 \times k_{obs} \times t$, where C is the nitrate concentration at time t, C_0 is the initial concentration of NO_3^-, and k_{obs} is the apparent NRR constant.

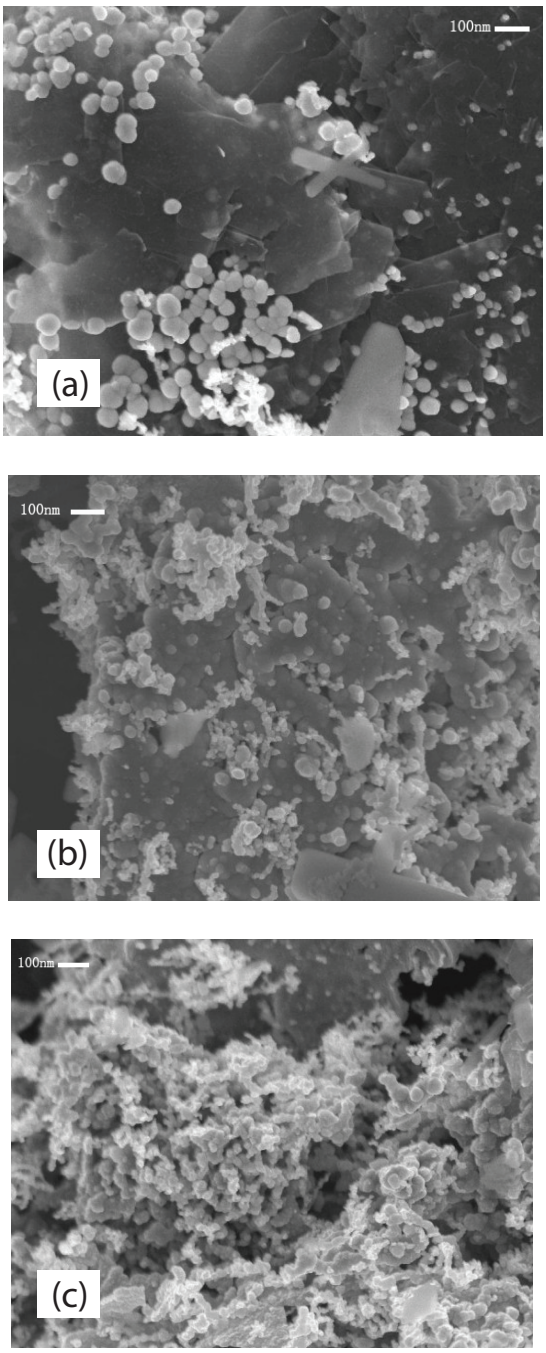

Fig. 14. SEM images of graphene loaded with iron nanoparticles before and after reaction with nitrate in simulated groundwater (A) 0 min, (B) 30 min, and (C) 90 min.

3.4.1. Effect of initial NO_3^- concentration on NRR

Table 3 shows that changes to the initial concentration of NO_3^- cause different NRRs. With increasing NO_3^- concentrations, the k_{obs} value tends to decrease from 0.20 to 0.12 (Table 3). Owing to the adsorption function, both reactive sites and non-reactive site were present on the surface of G-Fe composites during reaction with nitrates [21,28]. Because the k_{obs} varied with different initial concentrations of NO_3^-, we obtained different reaction kinetics (Table 3). This may be due to competition between nitrates for the limited number of reaction sites on the NZVI surface. Because the process of G-Fe removing nitrates included both adsorption and redox reactions. Therefore, the reaction kinetics equation was not a simple first-order reaction kinetics model.

3.4.2. Effect of pH on NRR

Table 4 shows that with increasing pH from 5.92 to 11.31, the k_{obs} value fluctuates in the range of 0.25–0.27, while at pH 2.15, the k_{obs} is elevated more obviously to 0.51. The results indicate that low pH level promotes nitrate reduction and denitrification reaction, thereby reducing the deposits on the surface of G-Fe, and providing fresher reaction sites for the chemical reaction. Altogether, these conditions promote the reduction of nitrates and improve the NRR [22,34].

3.4.3. Effect of DO on NRR

Table 5 demonstrates that an increase in DO causes minor variation in the k_{obs} (0.16–0.18). The k_{obs} value fluctuates in the range of 0.16–0.18 with increasing DO from 0.57 to 10.03. The result indicates that the effect of DO was negligible for the NRR during nitrate removal by G-Fe, which is an advantage of this composite material.

3.4.4. Effect of coexisting anions on NRR

Table 6 reveals that the addition of Cl^- or SO_4^{2-} causes a decrease in the k_{obs}; the effect of SO_4^{2-} was more obvious than Cl^-. These results indicate that the presence of coexisting anions reduces the NRR of nitrate removal.

3.4.5. Relationship between environmental factors and reaction rate constant

Within the ranges of the environmental factors tested, the k_{obs} value shows different levels of variation (Table 7). The greatest variation (0.26) of k_{obs} is associated with pH change (2.15–11.31). The degree to which these environmental factors affect the k_{obs} was as follows: pH > initial NO_3^- > coexistence anions (Cl^- and SO_4^{2-}) > DO.

Table 2
Reaction rate equation of nitrate removal by graphene loaded with iron nanoparticles at different load ratios of graphene and iron nanoparticles

Load ratio	Reaction order (n)	k_{obs} (mg-N/L)$^{1-n}$/min	Correlation coefficient (R^2)	Rate equation
2.5	0.38	0.97	0.9461	$-d[NO_3^-]/dt = 0.97 \times [NO_3^-]^{0.38}$
5.0	0.45	0.69	0.9762	$-d[NO_3^-]/dt = 0.69 \times [NO_3^-]^{0.45}$
7.5	1.08	0.10	0.9672	$-d[NO_3^-]/dt = 0.10 \times [NO_3^-]^{1.08}$
15	0.69	0.20	0.9506	$-d[NO_3^-]/dt = 0.20 \times [NO_3^-]^{0.69}$

Table 3
Reaction rate equation of nitrate removal by graphene loaded with iron nanoparticles at different initial concentrations of NO_3^- in simulated groundwater

Initial NO_3^- (mg/L)	k_{obs} (mg-N/L)$^{1-n}$/min	Correlation coefficient (R^2)	Rate equation
30	0.20	0.9902	$-d[NO_3^-]/dt = 0.20 \times [NO_3^-]^{0.45}$
50	0.19	0.9675	$-d[NO_3^-]/dt = 0.19 \times [NO_3^-]^{0.45}$
80	0.16	0.9450	$-d[NO_3^-]/dt = 0.16 \times [NO_3^-]^{0.45}$
120	0.12	0.8856	$-d[NO_3^-]/dt = 0.12 \times [NO_3^-]^{0.45}$

Table 4
Reaction rate equation of nitrate removal by graphene loaded with iron nanoparticles at different pH in simulated groundwater

pH	k_{obs} (mg-N/L)$^{1-n}$/min	Correlation coefficient (R^2)	Rate equation
2.15	0.51	0.8315	$-d[NO_3^-]/dt = 0.51 \times [NO_3^-]^{0.45}$
5.92	0.26	0.8475	$-d[NO_3^-]/dt = 0.26 \times [NO_3^-]^{0.45}$
7.03	0.27	0.9411	$-d[NO_3^-]/dt = 0.27 \times [NO_3^-]^{0.45}$
8.90	0.27	0.8095	$-d[NO_3^-]/dt = 0.27 \times [NO_3^-]^{0.45}$
11.31	0.25	0.6513	$-d[NO_3^-]/dt = 0.25 \times [NO_3^-]^{0.45}$

Table 5
Reaction rate equation of nitrate removal by graphene loaded with iron nanoparticles by different concentrations of dissolved oxygen in simulated groundwater

DO (mg/L)	k_{obs} (mg-N/L)$^{1-n}$/min	Correlation coefficient (R^2)	Rate equation
0.57	0.18	0.9007	$-d[NO_3^-]/dt = 0.18 \times [NO_3^-]^{0.45}$
4.54	0.17	0.9494	$-d[NO_3^-]/dt = 0.17 \times [NO_3^-]^{0.45}$
6.27	0.16	0.8801	$-d[NO_3^-]/dt = 0.16 \times [NO_3^-]^{0.45}$
10.03	0.17	0.8806	$-d[NO_3^-]/dt = 0.17 \times [NO_3^-]^{0.45}$

Table 6
Reaction rate equation of nitrate removal by graphene loaded with iron nanoparticles in the presence of coexisting anions in simulated groundwater

Coexisting anion	k_{obs} (mg-N/L)$^{1-n}$/min	Correlation coefficient (R^2)	Rate equation
None	0.27	0.7779	$-d[NO_3^-]/dt = 0.27 \times [NO_3^-]^{0.45}$
Cl^-	0.25	0.8089	$-d[NO_3^-]/dt = 0.25 \times [NO_3^-]^{0.45}$
SO_4^{2-}	0.21	0.8821	$-d[NO_3^-]/dt = 0.21 \times [NO_3^-]^{0.45}$

Table 7
Variations in the reaction rate of nitrate removal by graphene loaded with iron nanoparticles in simulated groundwater due to different environmental factors

Factor	Range	k_{obs}	k_{obs} variation
Initial NO_3^-	30–120 mg/L	0.12–0.20	0.08
pH	2.15–11.31	0.25–0.51	0.26
Dissolved oxygen	0.57–10.03 mg/L	0.16–0.18	0.02
Coexisting anions	None, Cl^-, SO_4^{2-}	0.21–0.27	0.06

4. Conclusions

This study showed that compare with NZVI, G-Fe had higher removal efficiency of nitrates in simulate groundwater. Under the same reaction conditions and dosing level, G-Fe achieved higher reaction rate and removal efficiency of nitrates, with a lower production rate of ammonia. The G-Fe composites synthesized in this study demonstrated good effects in removing of nitrate from simulated groundwater. The highest removal efficiency was obtained at the load ratio of graphene and NZVI of less than or equal to 5:1 and more than 90% nitrate was rapidly removed in 30 min. Irrespective of the pH level, G-Fe removed more than 75% nitrates under

the experimental conditions. Moreover, the coexisting anion PO_4^{3-} exhibited a great impact on the removal efficiency of nitrates and pretreatment of high PO_4^{3-} water samples is necessary for application of G-Fe. As the reaction proceeded, the nanoparticulate iron was gradually consumed and became flocculent. The complex process of nitrate removal involved a set of redox reactions and adsorption process. In view of these results, G-Fe prove advantageous at removing nitrates and offer a great potential to the removal of other contaminants in groundwater. This study provides technical support for engineering practice of groundwater nitrate pollution remediation. It is of scientific significance for exploration into new types of composite materials.

Acknowledgments

This study was supported by the National Natural Science Foundation of China (Nos. 41672224, 41471420, and 41703093), the Fundamental Research Funds for the Central Universities (Nos. GK201703052 and GK201701010) the China Postdoctoral Science Foundation (No. 2017M613048) and Shaanxi postdoctoral research funding project in China (No. 2017BSHTDZZ03).

References

[1] X. Quan, X. Ruan, H. Zhao, S. Chen, Y. Zhao, Photoelectrocatalytic degradation of pentachlorophenol in aqueous solution using a TiO_2 nanotube film electrode, Environ. Pollut., 147 (2007) 409–414.
[2] K.S. Haugen, M.J. Semmens, P.J. Novak, A novel in situ technology for the treatment of nitrate contaminated groundwater, Water Res., 36 (2002) 3497–3506.
[3] M.R. Schnobrich, B.P. Chaplin, M.J. Semmens, P.J. Novak, Stimulating hydrogenotrophic denitrification in simulated groundwater containing high dissolved oxygen and nitrate concentrations, Water Res., 41 (2007) 1869–1876.
[4] J.L. Costa, H. Massone, D.M. Artinez, E.E. Suero, C.M. Vidal, F. Bedman, Nitrate contamination of aquifer and accumulation in the unsaturated zone, Agric. Water Manage., 57 (2002) 33–47.
[5] M. Busch, W. Schmidt, V. Migunov, A. Beckel, C. Notthoff, A. Kompch, U. Winterer, M. Atakan, B. Bergmann, Effect of preparation of iron-infiltrated activated carbon catalysts on nitrogen oxide conversion at low temperature, Appl. Catal., B, 160–161 (2014) 641–650.
[6] H. Zhang, Z. Jin, L. Han, C. Qin, Synthesis of nanoscale zero valent iron supported on exfoliated graphite for removal of nitrate, Trans. Nonferrous Met. Soc. China, 16 (2006) 345–349.
[7] Y. Zhang, Y.M. Li, J.F. Li, L.J. Hu, X.M. Zheng, Enhanced removal of nitrate by a novel composite: nanoscale zero valent iron supported on pillared clay, Chem. Eng. J., 171 (2011) 526–531.
[8] Z. Feleke, Y. Sakakibara, A bio-electrochemical reactor coupled with adsorber for the removal of nitrate and inhibitory pesticide, Water Res., 36 (2002) 3092–3102.
[9] S.G. Cameron, L.A. Schipper, Nitrate removal and hydraulic performance of organic carbon for use in denitrification beds, Ecol. Eng., 36 (2010) 1588–1595.
[10] W.P. Barber, D.C. Stuckey, Nitrogen removal in a modified anaerobic baffled reactor (ABR): denitrification, Water Res., 34 (2000) 2413–2418.
[11] L.J. Yuan, Z.H. Pan, T.M. Huang, Integrated assessment on groundwater nitrate by unsaturated zone probing and aquifer sampling with environmental tracers, Environ. Pollut., 171 (2012) 226–233.
[12] Y.X. Ren, L. Yang, X. Liang, The characteristics of a novel heterotrophic nitrifying and aerobic denitrifying bacterium, *Acinetobacter junii* YB, Bioresour. Technol., 171 (2014) 1–9.
[13] Z. Shi, Y. Zhang, J.T. Zhou, M.X. Chen, X.J. Wang, Biological removal of nitrate and ammonium under aerobic atmosphere by *Paracoccus versutus* LYM, Bioresour. Technol., 148 (2013) 144–148.
[14] P.C. Mishra, R.K. Patel, Use of agricultural waste for the removal of nitrate-nitrogen from aqueous medium, J. Environ. Manage., 90 (2009) 519–522.
[15] P.M. Ayyasamy, S. Rajakumar, M. Sathishkumar, K. Swaminathan, K. Shanti, P. Lakshmanaperumalsamy, S. Lee, Nitrate removal from synthetic medium and groundwater with aquatic macrophytes, Desalination, 242 (2009) 286–296.
[16] S.N. Milmile, J.V. Pande, S. Karmakar, A. Bansiwal, T. Chakrabarti, Equilibrium isotherm and kinetic modeling of the adsorption of nitrates by anion exchange Indion NSSR resin, Desalination, 276 (2011) 38–44.
[17] A.A. Hekmatzadeh, A. Karimi-Jashani, N. Talebbeydokhti, B. Klve, Modeling of nitrate removal for ion exchange resin in batch and fixed bed experiments, Desalination, 284 (2012) 22–31.
[18] A. Devadas, S. Vasudevan, F. Epron, Nitrate reduction in water: influence of the addition of a second metal on the performances of the Pd/CeO_2 catalyst, J. Hazard. Mater., 185 (2011) 1412–1417.
[19] J. Xu, Z.W. Hao, C.S. Xie, X.S. Lv, Y.P. Yang, X.H. Xu, Promotion effect of Fe^{2+} and Fe_3O_4 on nitrate reduction using zero-valent iron, Desalination, 284 (2012) 9–13.
[20] R.C. Della, V. Belgiorno, S. Meric, Overview of in-situ applicable nitrate removal processes, Desalination, 204 (2007) 46–62.
[21] S.Y. Li, Z.H. Jin, X.Q. Jin, L. Zhou, T.L. Li, H. Zhang, Y.F. Zhu, Removal of nitrate in groundwater by zero-valent iron packed columns, J. Agro-Environ. Sci., 23 (2004) 1203–1206.
[22] H.Y. Li, W. Wang, Z.H. Jin, H. Zhang, X.M. Xuan, T.L. Li, Study on denitrification by synthesizing nanoscale zero-valent iron, Acta Scient. Natural Univ. Nankaiensis, 1 (2006) 8–13.
[23] Y. Hwang, D. Kim, H. Shin, Mechanism study of nitrate reduction by nano zero valent iron, J. Hazard. Mater., 185 (2011) 1513–1521.
[24] J. Guo, R. Wang, W.W. Tjiu, J.S. Pan, T.X. Liu, Synthesis of Fe nanoparticles@graphene composites for environmental applications, J. Hazard. Mater., 225–226 (2012) 63–73.
[25] S.X. Dong, X.M. Dou, D. Mohan, P. Charles, J.M. Luo, Synthesis of graphene oxide/schwertmannite nanocomposites and their application in Sb(V) adsorption from water, Chem. Eng. J., 270 (2015) 205–214.
[26] Z.J. Li, F. Chen, L.Y. Yuan, Y.L. Liu, Y.L. Zhao, Z.F. Chai, W.Q. Shi, Uranium adsorption on graphene oxide nanosheets from aqueous solutions, Chem. Eng. J., 210 (2012) 539–546.
[27] Z.J. Li, L. Wang, L.Y. Yuan, C.L. Xiao, L. Mei, L.R. Zheng, J. Zhang, J.H. Yang, Y.L. Zhao, Z.T. Zhu, Z.F. Chai, W.Q. Shi, Efficient removal of uranium from aqueous solution by zero-valent iron nanoparticle and its graphene composite, J. Hazard. Mater., 290 (2015) 26–33.
[28] H. Jabeen, V. Chandra, S. Jung, J.W. Lee, K.S. Kim, S.B. Kim, Enhanced Cr(VI) removal using iron nanoparticle decorated graphene, Nanoscale, 3 (2011) 3583–3585.
[29] Z.Q. Bai, Z.J. Li, C.Z. Wang, L.Y. Yuan, Z.R. Liu, J. Zhang, L.R. Zheng, Y.L. Zhao, Z.F. Chai, W.Q. Shi, Interactions between Th(IV) and graphene oxide: experimental and density functional theoretical investigations, RSC Adv., 4 (2014) 3340–3347.
[30] J. Liu, G. Liu, W. Liu, Preparation of water-soluble β-cyclodextrin/poly(acrylic acid)/graphene oxide nanocomposites as new adsorbents to remove cationic dyes from aqueous solution, Chem. Eng. J., 257 (2014) 299–308.
[31] W. Wang, Y.L. Cheng, T. Kong, G.S. Cheng, Iron nanoparticles decoration onto three-dimensional graphene for rapid and efficient degradation of azo dye, J. Hazard. Mater., 299 (2015) 50–58.
[32] Y. Zhao, S.K. Yang, G. Wang, M. Han, Adsorption behaviors of acetaminophen onto the colloid in sediment, Pol. J. Environ. Stud., 24 (2015) 853–861.
[33] G.C. Yang, H.L. Lee, Chemical reduction of nitrate by nanosized iron: kinetic and pathways, Water Res., 39 (2005) 884–894.

[34] Y.M. Li, Y. Zhang, J.F. Li, X.M. Zheng, Enhanced removal of pentachlorophenol by a novel composite: nanoscale zero valent iron immobilized on organobentonite, Environ. Pollut., 159 (2011) 3744–3749.
[35] J.K. Im, H.S. Son, K.D. Zoh, Perchlorate removal in Fe^0/H_2O systems: impact of oxygen availability and UV radiation, J. Hazard. Mater., 192 (2011) 457–464.
[36] Y. Lin, X. Cui, J. Bontha, Electrically controlled anion exchange. Based on polypyrrole and carbon nanotubes nanocomposite for perchlorate removal, Environ. Sci. Technol., 40 (2006) 4004–4009.